

Co-Seismic Effect of the 2011 Japan Earthquake on the Crustal Movement Observation Network of China

Shaomin Yang^{1,2}, Kai Tan¹, and Qi Wang^{2,3,*}

¹Key Laboratory of Earthquake Geodesy, Institute of Seismology, China Earthquake Administration, Wuhan, China

²Institute of Geophysics and Geomatics, China University of Geosciences, Wuhan, China

³Planetary Science Institute, China University of Geosciences, Wuhan, China

Received 28 February 2012, accepted 25 October 2012

ABSTRACT

Great earthquakes introduce measurable co-seismic displacements over regions of hundreds and thousands of kilometers in width, which, if not accounted for, may significantly bias the long-term surface velocity field constrained by GPS observations performed during a period encompassing that event. Here, we first present an estimation of the far-field co-seismic off-sets associated with the 2011 Japan M_w 9.0 earthquake using GPS measurements from the Crustal Movement Observation Network of China (CMONOC) in North China. The uncertainties of co-seismic off-set, either at cGPS stations or at campaign sites, are better than 5 - 6 mm on average. We compare three methods to constrain the co-seismic off-sets at the campaign sites in northeastern China 1) interpolating cGPS coseismic offsets, 2) estimating in terms of sparsely sampled time-series, and 3) predicting by using a well-constrained slip model. We show that the interpolation of cGPS co-seismic off-sets onto the campaign sites yield the best co-seismic off-set solution for these sites. The source model gives a consistent prediction based on finite dislocation in a layered spherical Earth, which agrees with the best prediction with discrepancies of 2 - 10 mm for 32 campaign sites. Thus, the co-seismic off-set model prediction is still a reasonable choice if a good coverage cGPS network is not available for a very active region like the Tibetan Plateau in which numerous campaign GPS sites were displaced by the recent large earthquakes.

Key words: GPS, CMONOC, Coseismic deformation, Tohoku-Oki earthquake

Citation: Yang, S., K. Tan, and Q. Wang, 2013: Co-seismic effect of the 2011 Japan earthquake on the Crustal Movement Observation Network of China. *Terr. Atmos. Ocean. Sci.*, 24, 531-540, doi: 10.3319/TAO.2012.10.25.01(TibXS)

1. INTRODUCTION

Refining present-day surface velocity fields using space-borne geodetic techniques like GPS, SLR and VLBI is among the important goals in lithospheric deformation studies because this is not only a prerequisite for quantitatively understanding its nature, distribution, amount and the mechanical processes that drive it (Holt et al. 2000), but is also critical for seismic risk assessment in earthquake prone regions. In China, much has been devoted in the past two decades to deploy national-wide densified GPS arrays by either continuous tracking or campaign-mode surveying to quantify the surface displacements associated with secular crustal deformation (Wang et al. 2001, 2003; Zhang et al. 2004; Gan et al. 2007; Qiao et al. 2007). So far, a total of

> 2000 survey-mode GPS sites and 260 continuous GPS stations have been in operation by the end of 2011 as a result of large scientific infrastructure implementation "Crustal Movement Observation Network of China (CMONOC)" (Niu et al. 2005; Li et al. 2012). The preliminary analysis of data acquired in 1998 - 2011 from the network indicates site displacement determination to be accurate to 2 mm yr⁻¹ for most of the campaign sites (Li et al. 2012). It is anticipated that the uncertainty in the current velocity field will steadily decrease as more GPS data, in particular cGPS data that proved useful in maintaining reference frame and reducing various sorts of systemic errors in the coordinate time series, are obtained in years to come. A more precise and detailed description of the ongoing deformation in different regions of China is an impending objective for those applying the CMONOC observations to continental dynamics studies

* Corresponding author
E-mail: wangqi@cug.edu.cn

and seeking clues to forecasting earthquake potential from meaningful spatio-temporal changes in the velocity field.

To this end, GPS data collected in a period as long as possible are required to minimize observation errors and resolve systematic signals. However, an effort to combine GPS data with a sufficient long history in a tectonic active region to infer its velocity field, assuming a linear trend in site displacements is sometimes challenged by intermittent major earthquakes. In China, moderate to great earthquakes (M_w 6 - 8) have occurred frequently in the past decade (e.g., Lasserre et al. 2005; Funning et al. 2007; Elliott et al. 2010; Wang et al. 2011b; Zhao et al. 2012) and even giant events $M_w \sim 9$ occur occasionally in neighboring regions (Chlieh et al. 2007; Simons et al. 2011). The stable crustal deformation process may be significantly disturbed by the earthquakes of various sizes that have introduced additional transient processes on different spatial scales. Thus, in most cases, GPS data collected at sites within or near epicentral zones are no longer valid for calculating their long-term averaged motion rates if a careful calibration cannot be applied. This is particularly true for the great Tohoku-Oki, Japan earthquake of 2011, which was generated by plate subduction mega-thrust rupture along part of the Japan Trench where the Pacific plate has under-thrust fast beneath northeast Japan to accommodate its northwestward motion (e.g., Sato et al. 2011; Simon et al. 2011). The far-field co-seismic deformation has definitely disturbed the long-term deformation pattern of North China (Wang et al. 2011a; Shestakov et al. 2012; Zhao et al. 2012; Zhou et al. 2012), posing serious problems to explore all GPS data to analyze the regional strain field associated with local tectonic activities (Li et al. 2012).

The co-seismic calibration applied to an affected GPS site can be estimated using three methods. First, the co-seismic off-set of a site is estimated simply from its position time series. At the worst case, two-epoch observations acquired respectively pre- and post-earthquakes must be analyzed together with a long-term site velocity determination. Second, it is interpolated from a cluster of isolated off-sets for nearby cGPS stations with the homogeneous co-seismic deformation field assumption. Finally, it can be predicted using a well-constrained source model inverted from geodetic or seismic data if the first two methods fail. In this paper we use a case study to investigate how to estimate co-seismic off-sets for campaign sites and assess their precision, aiming at minimizing the effects caused by the 2011 Japan M_w 9.0 mega-thrust earthquake on the local strain field estimation.

2. GPS MEASUREMENTS IN NORTH CHINA AND DATA ANALYSIS

The active tectonics in North China (Northeastern China, North China plain and Ordos) is governed by two major deformation processes, the subduction of the Pacific and

Philippine Sea plates to the east and the continental collision of the Indian and Eurasian plates to the west (Molnar and Tapponnier 1977). The deformation in this region is characterized by active rifting and subsiding sediment basins that cause widespread Cenozoic extension (Ye et al. 1987; Shen et al. 2000). This heavily populated region was the site of nine $M > 7$ events since 1600, an unusual manifestation of the present-day deformation. Crustal deformation measurements in North China were traced back to the late 1960s, aiming at earthquake deformation and assessment studies on earthquake potential in this region. GPS observations in this region were initiated in 1992 with a small-scale sparse network of geodetic pillar-type monuments installed for regular reoccupation (Shen et al. 2000). In the construction of CMONOC, GPS site density in North China is denser than anywhere else in China and surveys were regularly repeated at these sites (Niu et al. 2005; Li et al. 2012).

In 1999, the first-epoch campaign for ~ 1000 CMONOC campaign sites was conducted with 27 continuously tracking stations in operation (Wang et al. 2003). Since then regular repeated campaigns were made at a 2 - 3 year interval over the past decade. The fieldwork was implemented usually from March to August of the campaign year, in which each site was occupied for one session of 4 consecutive days using a dual-frequency GPS receiver equipped with a geodetic antenna at a 30 s sampling rate. In 2009 CMONOC was enhanced with the addition of 1000 campaign sites and 233 cGPS stations. Two survey epochs for a total of ~ 2000 sites were made respectively in 2009 and 2011 with a similar strategy, such as 4 consecutive day's occupation, dual-frequency GPS receiver equipped with a geodetic antenna at a 30 s sampling rate (Li et al. 2012). In 2011 the new-installed cGPS were put successively in use. One hundred thirty-eight cGPS stations were operating by the time of the 2011 great Japan earthquake (Wang et al. 2011a; Zhao et al. 2012).

Data analysis was done using the GIPSY-OASIS software package (Zumberg et al. 1997). The processing takes advantage of the CMONOC cGPS array in China and other IGS fiducial stations outside China (Li et al. 2012). GPS data obtained each day were processed separately to produce daily solutions containing coordinate estimates of all sites concerned. The data analysis used public data products including the JPL's precise satellite orbits, IGS antenna center models as well as the Earth's pole positions, drift rates and rotation rates. In the ionospheric-free inversion combination of L1/L2 carrier phase observables, the site coordinates were estimated simultaneously with carrier phase biases, receiver and satellite clock biases as white noise at every epoch and as random-walk variations in the zenith tropospheric delay and gradients at each site as well. The precise point positioning (PPP) approach is used in a sequential data cleaning for all sites to remove carrier phase cycle slips (Zumberg et al. 1997). In the final solution a network-mode strategy is adopted to resolve ambiguity as much as possible.

Our own daily solutions were combined with global IGS station daily solutions provided by JPL. The combined solutions were then all transformed into the ITRF2005 (Altamimi et al. 2007) using about 15 IGS core stations outside China (variable day to day) to define the 7 parameter Helmert transformation. For further analysis, we determined the velocity field in China by combining the 1999 - 2011 daily solutions into one singular solution using conventional least-squares, assuming a linear crustal motion everywhere. To avoid the co-seismic deformation associated with the 2011 event, post-earthquake daily solutions for the sites in North China were removed. The site velocities were estimated with a weighted least squares adjustment and then transformed the velocities into the Eurasia plate-fixed reference frame using a pole of rotation defined by the ITRF2005. This preliminary result does not contain any new sites. The resulting velocities are accurate to within 2 mm yr⁻¹ for most of the sites (Li et al. 2012). We restricted ourselves to using this long-term velocity field to remove inter-seismic components from the GPS position time series.

3. ESTIMATION OF CO-SEISMIC DEFORMATION CAUSED BY THE 2011 GREAT EARTHQUAKE

We estimated co-seismic off-sets at the 107 GPS sites

in North China all located at distances > 1300 kilometers from the earthquake epicenter. Daily position time series bracketing the day of the earthquake are used for the cGPS stations. The co-seismic off-sets are isolated by differencing the mean positions three days immediately before and after the earthquake. The site positions for the day of the earthquake were excluded from this calculation. Given that a mega-thrust earthquake occurred one thousand kilometers away, postseismic displacements can be totally ignored for a period of three days following the mainshock. The resulting co-seismic off-sets are accurate to within 2 - 3 mm for the horizontal components. This uncertainty was evaluated by propagating formal site coordinate errors extracted from the daily solutions. For comparison, the uncertainty in a quick solution of near-field co-seismic off-sets using a position time series sampled every five minutes (Simons et al. 2011) was estimated roughly at 1 - 2 centimeters. Our result is comparable in precision with data reported by Wang et al. (2011a) and Zhao et al. (2012) because we were analyzing almost the same data from the CMONOC but using various software packages and slightly different ways to detect the co-seismic signals.

In Fig. 1 we plot the time series in three coordinate components for two cGPS stations. The horizontal components of the co-seismic off-sets are easily identified by

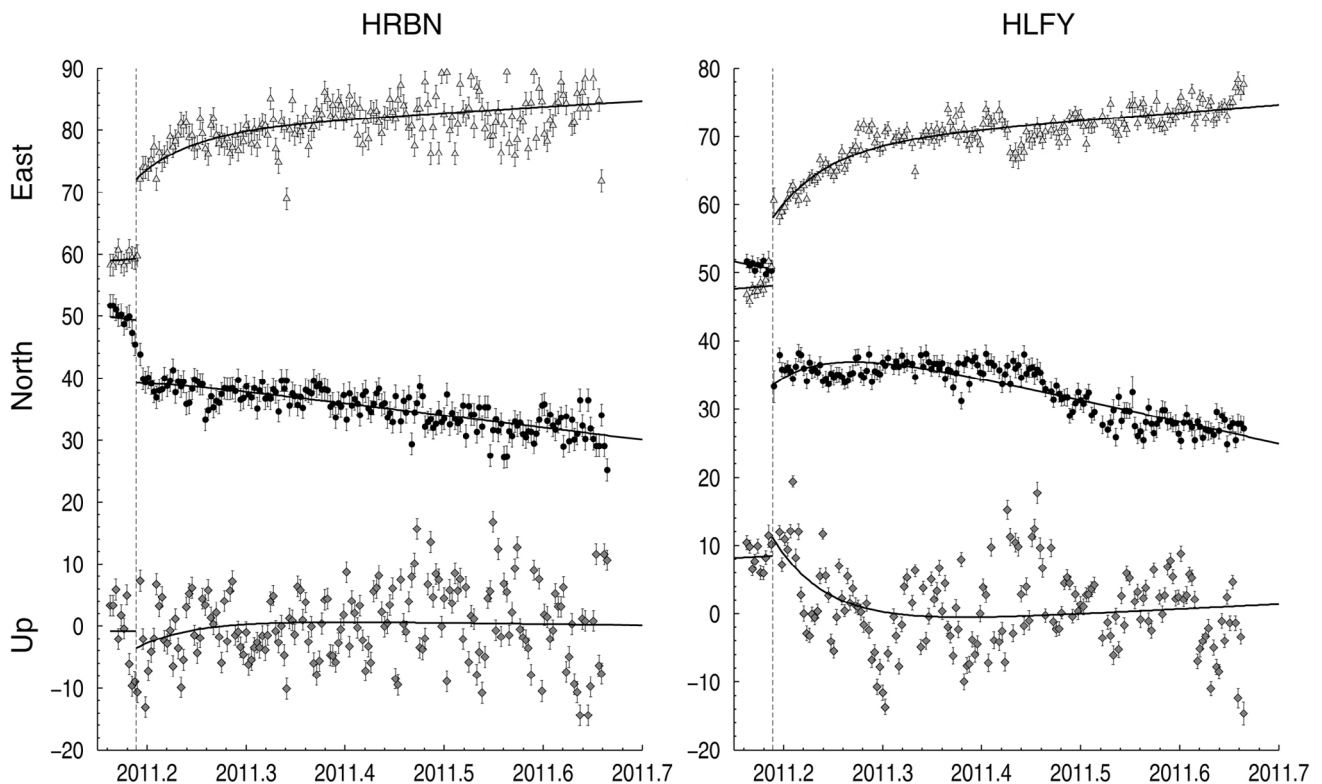


Fig. 1. Time series of two cGPS stations HRBI and HLFY (Fig. 2) in northeastern China for the 2011 Tohoku-Oki earthquake. The triangler, dots, and diamonds represent the east-west, north-south and vertical components of the coordinate time series in millimeter. The pre- and post-seismic positions are highlighted by offset curves. The dashed line denotes the event epoch.

visual inspection, whereas the vertical components are too smooth to be detected. In theory, the vertical signal is extremely weak in the far field and less than the uncertainty level at a distance of one thousand kilometers away from the epicenter. The far-field horizontal co-seismic displacement field is shown in Fig. 2. The cGPS stations in northeastern China (north of 40°N) documented co-seismic surface displacements up to 35 mm directed towards southeast, similar to the result from analyzing cGPS data in Far East Russia (Shestakov et al. 2012). The co-seismic displacements at the cGPS stations in the North China plain occur mostly within 10 mm directed roughly to the east. We are not aware of any sharp co-seismic displacement gradient across this region where active rifting is widely distributed (Ye et al. 1987). In fact, the observed co-seismic displacement declines gradually with distance away from the epicenter, as illustrated by Wang et al. (2011a) and Zhao et al. (2012). The GPS data quantified insignificant surface displacements in regions west of 110°E. In fact, the GPS-derived static off-sets there are statistically less than their uncertainties and are even not significantly different from zero. There is a coherent surface

motion roughly orienting toward the 600-km-long source zone at the Japan Trench.

We adopted two kinds of approaches to estimate the co-seismic off-sets at each GPS site. In the first approach the co-seismic off-sets are discriminated from each position time series, but sampled sparsely through a series of GPS campaigns. What is critical for this calculation is a pre-seismic velocity field that is estimated precisely from the pre-earthquake campaigns. A total of 357 campaign sites in this region are qualified with 4-epoch surveys from 1999 to 2009. The coseismic offsets are also estimated by differentiating the averaged positions at the earthquake epoch, which are propagated respectively forward and backward from the pre- and post-earthquake campaign results in terms of the pre-seismic velocity. The resolved off-sets have a typical uncertainty of 5 - 6 mm estimated from error propagation using the mean coordinate uncertainty of 2 - 3 mm and the pre-seismic velocity uncertainty of 2 - 3 mm yr⁻¹ multiplied by the time interval. Using this method the co-seismic offset uncertainties for the campaign sites might be larger by 1 - 2 factors than those for cGPS stations that do not invoke

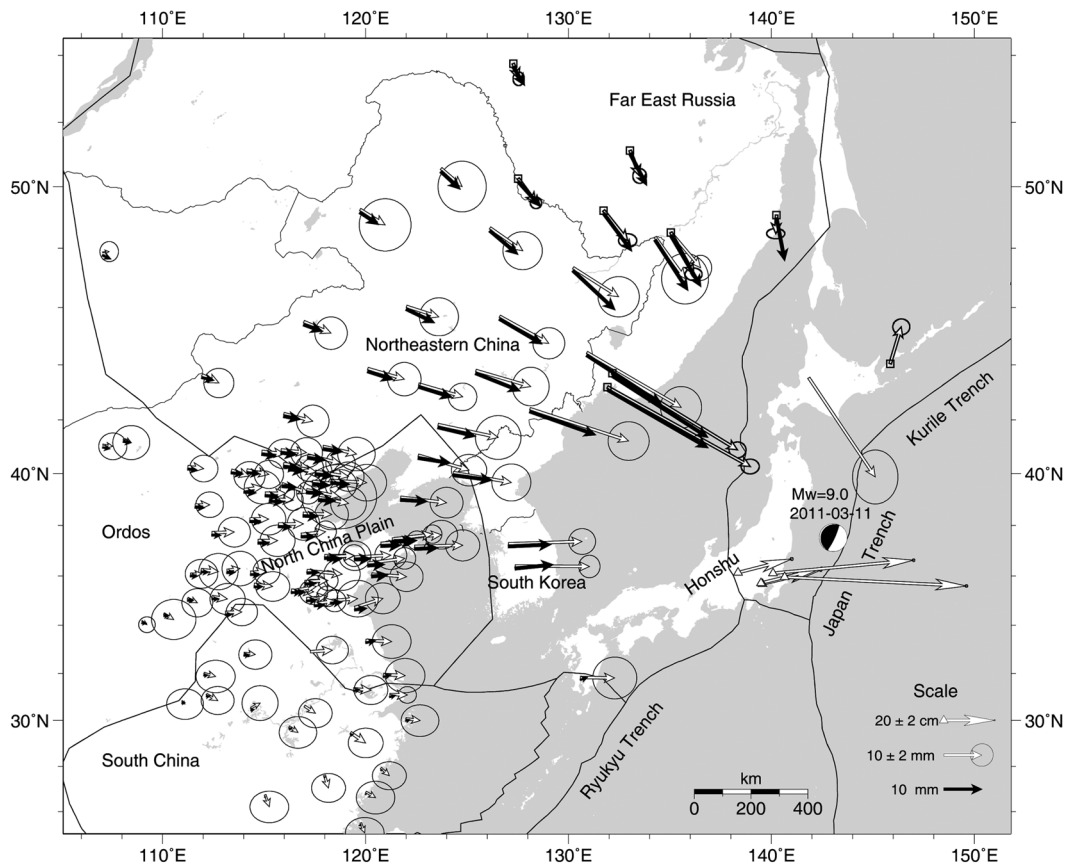


Fig. 2. The far-field co-seismic displacements associated with the 2011 Tohoku-Oki earthquake. The white arrows denote the horizontal displacements at cGPS stations inferred from GIPSY-derived position time series. The ellipses of the vectors are statistically in the 67% confidence level. The black arrows are predicted by our slip model. The square boxes are the cGPS stations reported by Shestakov et al. (2012). The stars represent two cGPS stations HRBN and HLFY. The triangles represent the near-field cGPS stations whose co-seismic displacements are displayed in a smaller scale for clarity.

any inter-seismic velocity calibration. For further assessment of these uncertainties, we adopted another approach - numerical interpolation, by which the co-seismic off-set for a specific campaign site is interpolated from a set of observed off-sets from 33 cGPS nearby stations. The interpolation of fitted cGPS off-set values onto a campaign site exploits bi-cubic Bessel functions (Holt et al. 2000). Such an indirect estimation is justified by a nearly continuous far-field deformation associated with the 2011 event and a good cGPS station coverage. Using this approach, co-seismic off-set uncertainties for most of the campaign sites in North China may be no larger than 4 mm, which is slightly better

than those based on the direct estimation from the sparsely sampled position time-series. Nevertheless, the overall pattern is very similar. We show two types of co-seismic off-sets for 32 campaign sites in northeastern China for evaluating their discrepancies in Fig. 3.

4. FAR-FIELD CO-SEISMIC OFF-SETS PREDICTED BY SOURCE MODELS

Co-seismic surface displacements due to the 2011 great earthquake were observed by more than 1200 cGPS sites distributed throughout the Japanese islands. The JPL

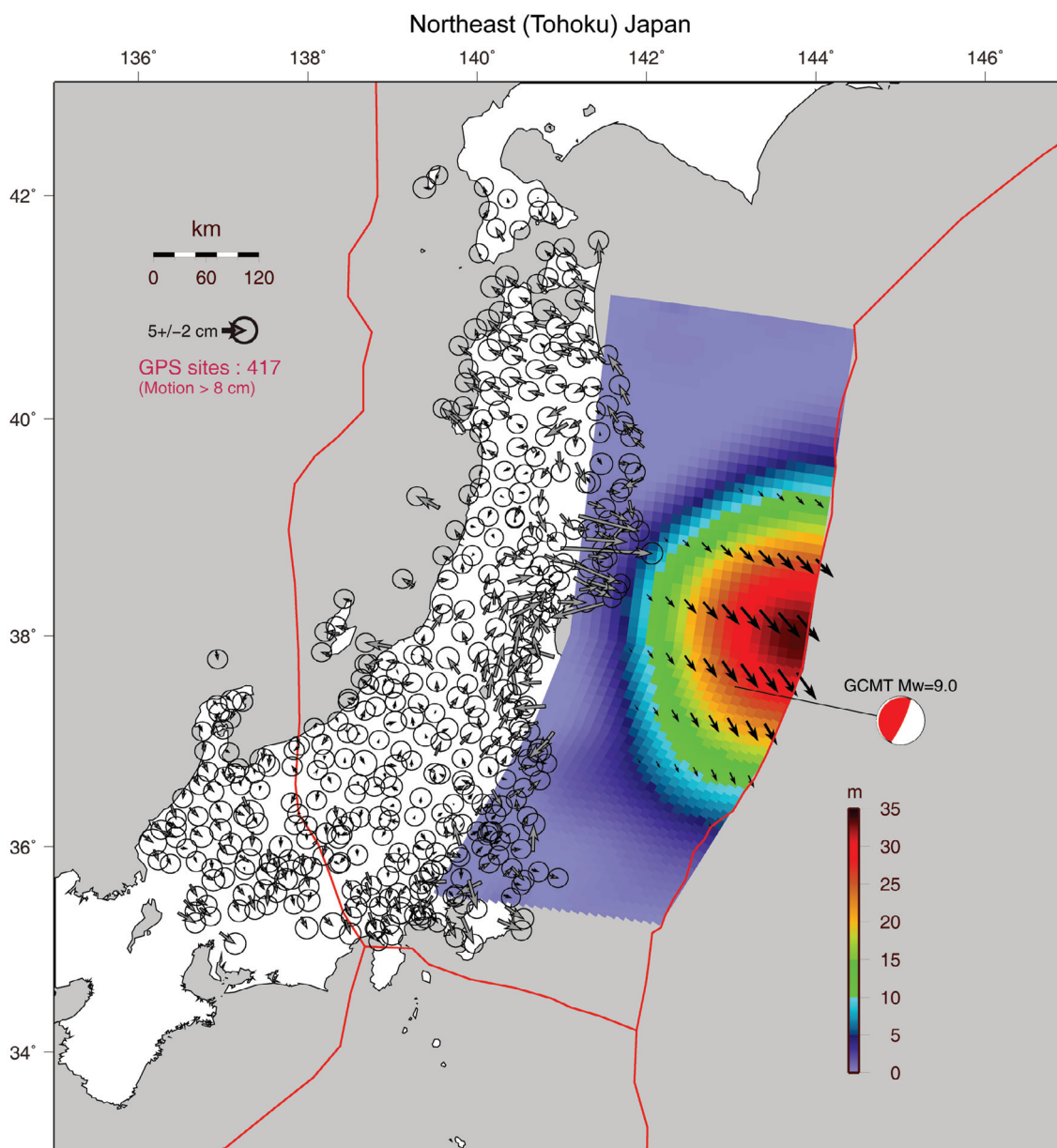


Fig. 3. The slip model inverted from the near-field GPS co-seismic displacements. The post-fit residuals (gray arrows) are displayed with error ellipses of 95% confidence. The slip magnitude on a patch is illustrated by the inserted color bar. The black arrows show the slip orientations of the high-slip patches.

team analyzed GPS data provided by the Geodetic Survey of Japan (GSI) using the GIPSY, which yielded a site position time series determined at a 5-min rate in a kinematic solution. The co-seismic off-sets were isolated from 2-epoch positions, respectively at 0540 and 0550 UTC. The original time for this event was 0546 UTC. Notable surface displacements are manifested over the entire northern half of Honshu (Fig. 4), with a maximum GPS off-set exceeding 5.2 m for the horizontal components and 1.2 m for the vertical. (Ozawa et al. 2011; Simons et al. 2011). Numerous slip models were inverted from this near-field geodetic dataset and the inverted models all showed a homogeneous and continuously distributed slip behavior (e.g., see Koketsu et al. 2011; Ozawa et al. 2011; Pollitz et al. 2011; Simon et al. 2011; Yue et al. 2011). Some of them are constrained with a slip distribution tapering to zero at the trench (Koketsu et al. 2011; Pollitz et al. 2011). Other inversions without this constraint find exceptionally large slip in this area (e.g., Simons et al. 2011; Yue et al. 2011). Nevertheless, all slip

models resolved a dominating thrusting motion that is confined mostly to the shallow portion above 25 km depth, and show that the slip propagated over a distance of 500 km along the strike of the mega-thrust fault.

In a similar way, we constructed source models of the 2011 event for evaluating its far-reaching effects on North China. The modeling is based on a geodetic inversion of the static off-sets provided by the JPL team together with a number of sea-floor displacements observed by acoustic/GPS combination on the hanging wall (Sato et al. 2011). The inversion is performed in terms of finite dislocation embedded in an elastic half space (Okada 1985). We adopted a fault plane roughly 660 km long by 250 km wide whose strike and dip angle of 10° are prescribed, which is consistent with the focal mechanism and the geometry of the plate boundary.

The plane for the earthquake rupture is further divided into 1650 rectangular patches 10 by 10 km in size. Following the geodetic inversion for the 2008 Wenchuan earthquake

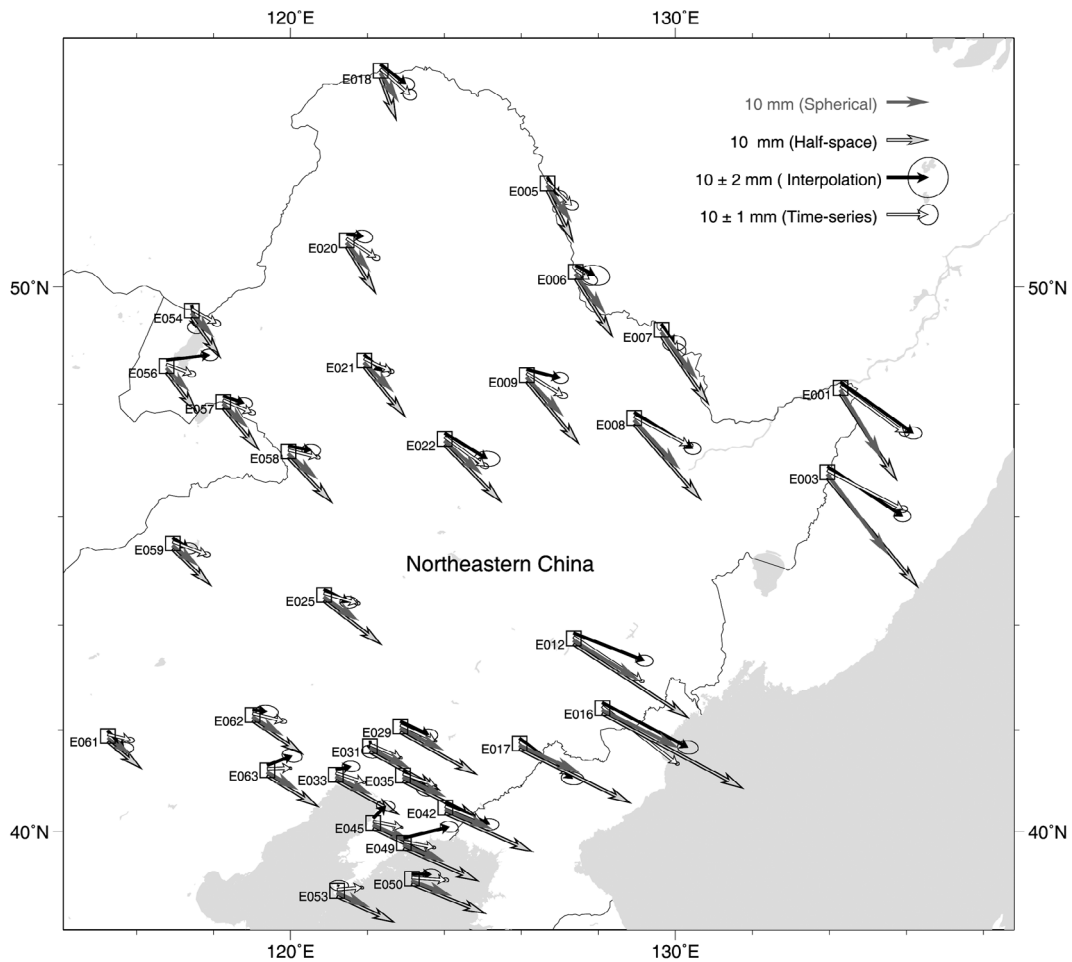


Fig. 4. The observed vs. modeled co-seismic off-sets at the CMONOC campaign sites in Northeastern China. The arrows are estimated from campaign data (white), interpolated from the cGPS co-seismic off-sets shown in Fig. 2 (black), and predicted by using the slip model shown in Fig. 3 assuming the finite dislocation respectively in a half-space (deep gray) as well as a layered Earth (light gray). The ellipses of the vectors are statistically in the 95% confidence level.

(Wang et al. 2011b), we tried to use the non-negative least-squares and bounded variable least-squares algorithms to resolve the slip on the model plane. Based on a total of 418 GPS vectors with amplitudes greater than 8 cm we solved for the slip distribution of the observed data by minimizing their postfit residuals and preserving the slip smoothness on the patches. The overall misfit of the resulting model is 4.2 cm with a smoothness weighting of 32 imposed. The total geodetic moment released by the event is estimated to 4.01×10^{22} Nm, assuming a rigidity of 40 Gpa, corresponding to a moment magnitude of $M_w = 9.0$. The slip model defines a compact pattern of thrusting motion with most slip occurring around the epicenter with a peak of 35 meters at the trench using the non-negative least-squares. If a smoothing factor of 16 is imposed, the peak slip is increased to 50 m (see Fig. 3).

The previous slip models based on geodetic data alone or combined with seismic data resolving peak slips in a range of 20 - 80 meters localized either near to or somewhat landward away from the trench. Note that the slip distribution offshore is too difficult to be resolved using the on-shore geodetic data. Usually the rupture details on the up-dip tip of a plate interface are obscured because few geodetic data were acquired on the hanging wall near the trench (Sato et al. 2011). The situation is more serious in the case of the 2011 event by the fact that the GPS sites are all on one side (~200 km) far from the trench. Thus, we fit the same data set equally well using the bounded variable least-squares with upper limit set to be 10 - 20 meters, resulting in a slip distribution whose high-slip patches lie close to the epicenter. Nonetheless, the first-order characteristics (seismic moment, rupture length, and asperity geometry etc.) derived from our modeling of the data onshore is sufficiently robust to meet our requirements for the estimation of surface displacements in affected regions as far as North China. Thus, we paid little attention to modeling details in this study.

The co-seismic displacements are predicted at the cGPS sites and campaign sites in northeastern China (see Fig. 2). In doing this we utilized two different methods with consideration of the curvature of Earth (Sun et al. 1996) or not (Okada 1985). In the former, we used the slip model to calculate the co-seismic off-sets based on the spherical dislocation theory in which the PREM model for stratified elastic isotropic Earth is adopted (Dziewonski and Anderson 1981). In the latter, the far-field co-seismic off-sets are actually computed from Okada's formula with the model parameters. The model off-sets in a layered Earth show a deformation pattern similar to the observed and our calculation for the cGPS stations in northeast China is not significantly different than the result reported by Zhou et al. (2012). The modeled and observed values converge to 2 - 6 mm (with a RMS misfit of 3 mm) for the 33 cGPS stations in northeastern China. The model values are all less than the observed in magnitude. The maximum discrepancy of

10 mm is found at SUIY, the nearest cGPS station in China to the earthquake source (Fig. 2). To east, 13 - 15 mm of misfits are found at VALD and GRNC in Far East Russia. The maximum misfits at three cGPS stations are one-third of the observed off-sets. Such larger misfits in the far-field are actually comparable to near-field misfits that may be attributed to an imprecise slip model and unrealistic assumptions about the structure of the Earth.

We compared two sets of model values at the cGPS stations predicted respectively by the half-space and spherical dislocation methods using the same slip model (Fig. 3). Note that the spherical method gives a perfect agreement with the observed coseismic displacements within 2-sigma uncertainties (Fig. 4). Only a few stations in the easternmost region show a minor underestimation by 7 - 8 mm at maximum if compared to the observed offsets, whereas the half-space method leads to an overall overestimation of up to 15 mm. It is obvious that the half-space method that ignores the Earth's curvature introduced additional biases to the misfits in the far-field over a distance of 1000 - 2000 km from the source.

We compared the interpolated and estimated off-sets at the campaign sites with those predicted by using the methods mentioned above. The result given by the spherical method shows an overall agreement to 2 - 6 mm in amplitude with the observed offsets for most of the 32 campaign sites (Fig. 5). The comparison yields a RMS misfit of 3 - 4 mm between them. Note that the discrepancies between the interpolated and observed off-sets converge to 2 - 4 mm for these sites, which is merely marginally better than that between the modeled and observed off-sets. However, the model off-sets rotate clockwise by $10^\circ - 60^\circ$ relative to the observed, whereas the interpolated and observed off-sets have almost identical directions. The half-space method yielded a RMS misfit of 5 - 6 mm, which is slightly worse than the statistics in the spherical method.

5. DISCUSSION AND CONCLUSION

The intensive geodetic observations in the near- and far-field for the 2011 great Japan earthquake provided an excellent chance to test various methods for calculating the far-field effect in a relatively stable, intensively studied region. Our study for the 2011 event could give some guidelines in applying various methods to estimate co-seismic off-sets at campaign sites affected by large remote earthquakes.

From our case study the far-field co-seismic effect can be derived by numerically interpolating the co-seismic displacements of nearby cGPS stations. The high-precision solution from a dense cGPS network is actually free of model assumption (e.g., inter-seismic or post-seismic processes), therefore it is qualified to define a co-seismic displacement field for the affected area. By adopting a simple assumption,

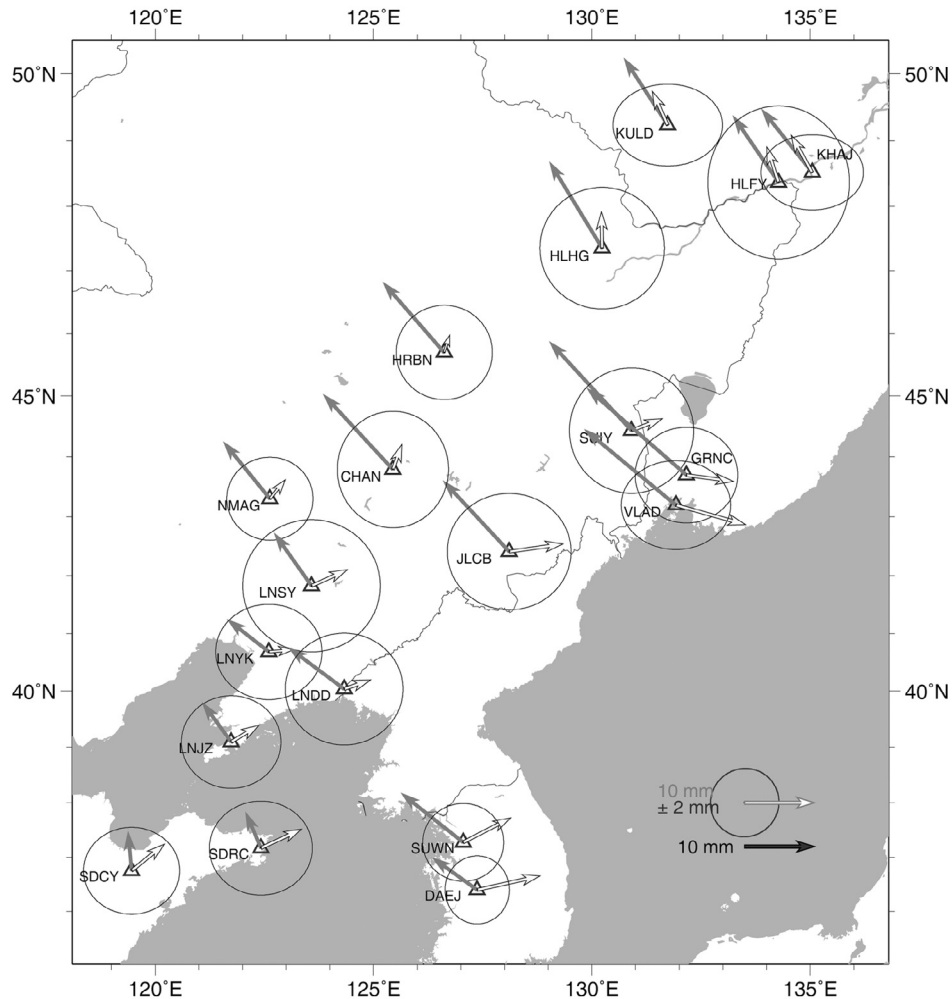


Fig. 5. The modeled co-seismic off-sets at the CMONOC cGPS stations. The white and gray arrows show the co-seismic off-sets predicted by the layered spherical dislocation and homogenous half-space dislocation, respectively. The ellipses represent the formal errors in cGPS co-seismic off-sets with a 95% confidence level.

interpolating the cGPS co-seismic displacements onto any campaign site lying within the cGPS network is a better choice, at least no worse than estimating the co-seismic off-set from a sparsely sampled time series. We explored this strategy to remove the co-seismic effect associated with the 2011 great Japan earthquake from the CMONOC campaign sites in North China for a long-term surface velocity field. With such estimated off-sets the post-earthquake GPS position time series could be used to derive site velocities for most CMONOC sites in this region with the available two-epoch surveys (Li et al. 2012).

Unfortunately, such a good condition for earthquake monitoring is rarely applied elsewhere in China. In the past decade the Tibetan Plateau and its margins were subjected to several major earthquake strikes - the 2001 Kokoxili M_w 7.8 earthquake, 2008 Yutian M_w 7.1 earthquake, 2008 Wenchuan M_w 7.9 earthquake, and 2010 Yushu M_w 6.9 earthquake. It was noted that the 2004 great Sumatra earthquake produced far-field co-seismic offsets at CMONOC sites in

southwest China (Fu and Sun 2006; Qiao et al. 2007). Few cGPS stations were in operation at that time in broad areas affected by these events. Fortunately most of these large earthquakes were intensively studied with InSAR interferograms (Lasserre et al. 2005; Funning et al. 2007; Hashimoto et al. 2010; Zha et al. 2011) and a few were investigated by using either near-field GPS measurements (Chlieh et al. 2007) or both InSAR and GPS data (Wang et al. 2011b). As a result, slip models of these events are usually constrained well with resolved details and may be sufficient for our needs. Based on this study, the slip model of a great earthquake if constrained well by near-field geodetic data may provide the solid ground necessary to estimate co-seismic off-sets to within an uncertainty of, to say, 5 - 10 mm for far-field campaign sites.

Obviously, for the campaign sites located away from the epicenters over distances of a few thousand kilometers, the method based on a homogeneous half-space dislocation could not address this end. In our study the method based on

dislocation in the half-space tends to overestimate far-field static off-set. Meanwhile in a numerical test on slip models of the 2004 great Sumatra earthquake, the associated far-field displacements tended to become larger in the homogeneous half-space than in the layered spherical Earth (Banerjee et al. 2005). Thus, for the CMONOC sites in southwest China a layered spherical Earth with the refined slip model (e.g., Chlieh et al. 2007) should be considered to simulate the far-field off-sets associated with the 2004 event.

It is worthwhile to implement such an estimation based on either the half-space (e.g., 2001 Kokoxili and 2008 Wenchuan earthquakes) or the layered spherical Earth (e.g., 2004 Sumatra earthquake) because the inter-seismic velocity rates of campaign sites are usually not well constrained by limited observations. The far-field co-seismic off-sets estimated from sparsely sampled position time-series may be biased by imprecise inter-seismic rates and frequent moderate M_w 5 - 6 earthquakes nearby. Model co-seismic off-sets with an uncertainty of 5 - 10 mm on average are still useful in deriving a decade long velocity field for very active regions characterized by high velocity rates of > 10 mm, such as the Tibetan Plateau and Tien Shan (Wang et al. 2001; Zhang et al. 2004; Gan et al. 2007; Qiao et al. 2007; Yang et al. 2008). On the contrary, it may be more reasonable to estimate co-seismic off-sets from the time series for sites in stable regions with internal deformation of < 3 mm yr⁻¹ such as North China and South China (Li et al. 2012).

Acknowledgements The authors thank the CMONOC project for providing us GPS data. W. K. Sun provided us the spherical dislocation code. We are grateful to the two anonymous reviewers whose comments improved this paper and for technical support from G. Y. Fu. This work is funded by the NSFC through grants No. 40674054 and 41074016 to the authors.

REFERENCES

- Altamimi, Z., X. Collilieux, J. Legrand, B. Garayt, and C. Boucher, 2007: ITRF2005: A new release of the International Terrestrial Reference Frame based on time series of station positions and Earth Orientation Parameters. *J. Geophys. Res.*, **112**, B09401, doi: 10.1029/2007JB004949. [[Link](#)]
- Banerjee, P., F. F. Pollitz, and R. Bürgmann, 2005: The size and duration of the Sumatra-Andaman earthquake from far-field static offsets. *Science*, **308**, 1769-1772, doi: 10.1126/science.1113746. [[Link](#)]
- Chlieh, M., J.-P. Avouac, V. Hjørleifsdóttir, T.-R. A. Song, C. Ji, K. Sieh, A. Sladen, H. Hebert, L. Prawirodirdjo, Y. Bock, and J. Galetzka, 2007: Coseismic slip and afterslip of the great M_w 9.15 Sumatra-Andaman earthquake of 2004. *Bull. Seismol. Soc. Am.*, **97**, S152-S173, doi: 10.1785/0120050631. [[Link](#)]
- Dziewonski, A. M. and D. L. Anderson, 1981: Preliminary reference earth model. *Phys. Earth Planet. Inter.*, **25**, 297-356, doi: 10.1016/0031-9201(81)90046-7. [[Link](#)]
- Elliott, J. R., R. J. Walters, P. C. England, J. A. Jackson, Z. Li, and B. Parsons, 2010: Extension on the Tibetan plateau: Recent normal faulting measured by InSAR and body wave seismology. *Geophys. J. Int.*, **183**, 503-535, doi: 10.1111/j.1365-246X.2010.04754.x. [[Link](#)]
- Fu, G. and W. Sun, 2006: Global coseismic displacements caused by the 2004 Sumatra-Andaman earthquake (M_w 9.1). *Earth Planets Space*, **58**, 149-152.
- Funning, G. J., B. Parsons, and T. J. Wright, 2007: Fault slip in the 1997 Manyi, Tibet earthquake from linear elastic modelling of InSAR displacements. *Geophys. J. Int.*, **169**, 988-1008, doi: 10.1111/j.1365-246X.2006.03318.x. [[Link](#)]
- Gan, W., P. Zhang, Z. K. Shen, Z. Niu, M. Wang, Y. Wan, D. Zhou, and J. Cheng, 2007: Present-day crustal motion within the Tibetan Plateau inferred from GPS measurements. *J. Geophys. Res.*, **112**, B08416, doi: 10.1029/2005JB004120. [[Link](#)]
- Hashimoto, M., M. Enomoto, and Y. Fukushima, 2010: Coseismic deformation from the 2008 Wenchuan, China, earthquake derived from ALOS/PALSAR Images. *Tectonophysics*, **491**, 59-71, doi: 10.1016/j.tecto.2009.08.034. [[Link](#)]
- Holt, W. E., N. Chamot-Rooke, X. L. Pichon, A. J. Haines, B. Shen-Tu, and J. Ren, 2000: Velocity field in Asia inferred from Quaternary fault slip rates and Global Positioning System observations. *J. Geophys. Res.*, **105**, 19185-19209, doi: 10.1029/2000JB900045. [[Link](#)]
- Koketsu, K., Y. Yokota, N. Nishimura, Y. Yagi, S. Miyazaki, K. Satake, Y. Fujii, H. Miyake, S. Sakai, Y. Yamanaoka, and T. Okada, 2011: A unified source model for the 2011 Tohoku earthquake. *Earth Planet. Sci. Lett.*, **310**, 480-487, doi: 10.1016/j.epsl.2011.09.009. [[Link](#)]
- Lasserre, C., G. Peltzer, F. Crampé, Y. Klinger, J. Van der Woerd, and P. Tapponnier, 2005: Coseismic deformation of the 2001 $M_w = 7.8$ Kokoxili earthquake in Tibet, measured by synthetic aperture radar interferometry. *J. Geophys. Res.*, **110**, doi: 10.1029/2004JB003500. [[Link](#)]
- Li, Q., X. You, S. Yang, R. Du, X. Qiao, R. Zou, and Q. Wang, 2012: A precise velocity field of tectonic deformation in China as inferred from intensive GPS observations. *Sci. China Earth Sci.*, **55**, 695-698, doi: 10.1007/s11430-012-4412-5. [[Link](#)]
- Molnar, P. and P. Tapponnier, 1977: Relation of the tectonics of eastern China to the India-Eurasia collision: Application of slip-line field theory to large-scale continental tectonics. *Geology*, **5**, 212-216, doi: 10.1130/0091-7613(1977)5<212:ROTTOT>2.0.CO;2. [[Link](#)]
- Niu, Z., M. Wang, H. Sun, J. Sun, X. You, W. Gan, G. Xue,

- J. Hao, S. Xin, Y. Wang, Y. Wang, and B. Li, 2005: Contemporary velocity field of crustal movement of Chinese mainland from Global Positioning System measurements. *Chin. Sci. Bull.*, **50**, 939-941. doi: 10.1007/BF02897392. [[Link](#)]
- Okada, Y., 1985: Surface deformation due to shear and tensile faults in a half-space. *Bull. Seismol. Soc. Am.*, **75**, 1135-1154.
- Ozawa, S., T. Nishimura, H. Suito, T. Kobayashi, M. Tobita, and T. Imakiire, 2011: Coseismic and postseismic slip of the 2011 magnitude-9 Tohoku-Oki earthquake. *Nature*, **475**, 373-376, doi: 10.1038/nature10227. [[Link](#)]
- Pollitz, F. F., R. Bürgmann, and P. Banerjee, 2011: Geodetic slip model of the 2011 M9.0 Tohoku earthquake. *Geophys. Res. Lett.*, **38**, L00G08, doi: 10.1029/2011GL048632. [[Link](#)]
- Qiao, X., S. Yang, R. Du, Q. Wang, K. Tan, and L. Guo, 2007: GPS-derived crustal deformation in southwestern China. *Aust. J. Earth Sci.*, **54**, 521-529, doi: 10.1080/08120090601075400. [[Link](#)]
- Sato, M., T. Ishikawa, N. Ujihara, S. Yoshida, M. Fujita, M. Mochizuki, and A. Asada, 2011: Displacement above the hypocenter of the 2011 Tohoku-Oki earthquake. *Science*, **332**, p 1395, doi: 10.1126/science.1207401. [[Link](#)]
- Shen, Z., C. Zhao, A. Yin, Y. Li, D. D. Jackson, P. Fang, and D. Dong, 2000: Contemporary crustal deformation in east Asia constrained by Global Positioning System measurements. *J. Geophys. Res.*, **105**, 5721-5734, doi: 10.1029/1999JB900391. [[Link](#)]
- Shestakov, N. V., H. Takahashi, M. Ohzono, A. S. Prytkov, V. G. Bykov, M. D. Gerasimenko, M. N. Luneva, G. N. Gerasimov, A. G. Kolomiets, V. A. Bormotov, N. F. Vasilenko, J. Baek, P.-H. Park, and M. A. Serov, 2012: Analysis of the far-field crustal displacements caused by the 2011 great Tohoku earthquake inferred from continuous GPS observations. *Tectonophysics*, **524-525**, 76-86, doi: 10.1016/j.tecto.2011.12.019. [[Link](#)]
- Simons, M., S. E. Minson, A. Sladen, F. Ortega, J. Jiang, S. E. Owen, L. Meng, J.-P. Ampuero, S. Wei, R. Chu, D. V. Helmberger, H. Kanamori, E. Hetland, A. W. Moore, and F. H. Webb, 2011: The 2011 magnitude 9.0 Tohoku-Oki earthquake: Mosaicking the megathrust from seconds to centuries. *Science*, **332**, 1421-1425, doi: 10.1126/science.1206731. [[Link](#)]
- Sun, W., S. Okubo, and P. Vaníček, 1996: Global displacements caused by point dislocations in a realistic earth model. *J. Geophys. Res.*, **101**, 8561-8577, doi: 10.1029/95JB03536. [[Link](#)]
- Wang, M., Z. Shen, Z. Niu, Z. Zhang, H. Sun, W. Gan, Q. Wang, and Q. Ren, 2003: Contemporary crustal deformation of the Chinese continent and tectonic block model. *Sci. China Ser. D: Earth Sci.*, **46**, 25-40.
- Wang, M., Q. Li, F. Wang, R. Zhang, Y. Wang, H. Shi, P. Zhang, and Z. Shen, 2011a: Far-field coseismic displacements associated with the 2011 Tohoku-oki earthquake in Japan observed by Global Positioning System. *Chin. Sci. Bull.*, **56**, 2419-2424, doi: 10.1007/s11434-011-4588-7. [[Link](#)]
- Wang, Q., P. Z. Zhang, J. T. Freymueller, R. Bilham, K. M. Larson, X. Lai, X. You, Z. Niu, J. Wu, Y. Li, J. Liu, Z. Yang, and Q. Chen, 2001: Present-day crustal deformation in China constrained by Global Positioning System measurements. *Science*, **294**, 574-577, doi: 10.1126/science.1063647. [[Link](#)]
- Wang, Q., X. Qiao, Q. Lan, J. Freymueller, S. Yang, C. Xu, Y. Yang, X. You, K. Tan, and G. Chen, 2011b: Rupture of deep faults in the 2008 Wenchuan earthquake and uplift of the Longmen Shan. *Nat. Geosci.*, **4**, 634-640, doi: 10.1038/NCEO1210. [[Link](#)]
- Yang, S., J. Li, and Q. Wang, 2008: The deformation pattern and fault rate in the Tianshan Mountains inferred from GPS observations. *Sci. China Ser. D: Earth Sci.*, **51**, 1064-1080, doi: 10.1007/s11430-008-0090-8. [[Link](#)]
- Ye, H., B. Zhang, and F. Mao, 1987: The Cenozoic tectonic evolution of the Great North China: Two types of rifting and crustal necking in the Great North China and their tectonic implications. *Tectonophysics*, **133**, 217-227, doi: 10.1016/0040-1951(87)90265-4. [[Link](#)]
- Yue, H. and T. Lay, 2011: Inversion of high-rate (1 sps) GPS data for rupture process of the 11 March 2011 Tohoku earthquake (M_w 9.1). *Geophys. Res. Lett.*, **38**, L00G09, doi: 10.1029/2011GL048700. [[Link](#)]
- Zha, X., Z. Dai, L. Ge, K. Zhang, X. Li, X. Chen, Z. Li, and R. Fu, 2011: Fault geometry and slip distribution of the 2010 Yushu earthquakes inferred from InSAR measurement. *Bull. Seismol. Soc. Am.*, **101**, 1951-1958, doi: 10.1785/0120100192. [[Link](#)]
- Zhang, P. Z., Z. Shen, M. Wang, W. Gan, R. Bürgmann, P. Molnar, Q. Wang, Z. Niu, J. Sun, J. Wu, H. Sun, and X. You, 2004: Continuous deformation of the Tibetan Plateau from global positioning system data. *Geology*, **32**, 809-812, doi: 10.1130/G20554.1. [[Link](#)]
- Zhao, B., W. Wang, S. Yang, M. Peng, X. Qiao, R. Du, and Z. Nie, 2012: Far field deformation analysis after the M_w 9.0 Tohoku earthquake constrained by cGPS data. *J. Seismol.*, **16**, 305-313, doi: 10.1007/s10950-011-9271-6. [[Link](#)]
- Zhou, X., W. Sun, B. Zhao, G. Fu, J. Dong, and Z. Nie, 2012: Geodetic observations detecting coseismic displacements and gravity changes caused by the M_w = 9.0 Tohoku-Oki earthquake. *J. Geophys. Res.*, **117**, B05408, doi: 10.1029/2011JB008849. [[Link](#)]
- Zumberge, J. F., M. B. Heflin, D. C. Jefferson, M. M. Watkins, and F. H. Webb, 1997: Precise point positioning for the efficient and robust analysis of GPS data from large networks. *J. Geophys. Res.*, **102**, 5005-5017, doi: 10.1029/96JB03860. [[Link](#)]